Optical Properties of Asian Dust measured by Raman Lidar at Taipei, Taiwan

W. N. Chen[(1)], F. J. Tsai[(1)], Charles C. K. Chou[(1)], S. Y. Chang[(1)], T. K. Chen[(1)], J. P. Chen[(2)]

[(1)] *Research Center for Environmental Changes, Academia Sinica, Taiwan, wnchen@rcec.sinica.edu.tw*
[(2)] *Atmospheric Science Department, National Taiwan University, Taiwan, jpchen@as.ntu.edu.tw*

ABSTRACT

The optical properties and height distribution of spring aerosols measured by Lidar are reported. An Aerosol Regional Dust Model and HYSPLIT back-trajectory analysis were applied to identify the origin of dust layers. The results show most of the dust layers were located at height between 1 km and 5 km and could be observed quite frequently. The lidar ratios for 355 nm S_{355} distribute between 32 sr and 72 sr. The depolarization ratios vary from 2% to 25% and the backscattering ratios are about R_{532}=1.5-10. The correlations between particle depolarization and backscatter-related angstrom components were found usually negatively correlated and may be destroyed under higher relative humidity (RH>60%).

1. INTRODUCTION

When Taiwan is suffered by winter monsoon, aerosol with higher depolarization ratio (DP≈5-25%) could be frequently observed at height above boundary by a Raman/Depolarization lidar, which indicates the existence of non-spherical particles. HYSPLIT back-trajectory analysis shows almost all of the depolarization layers oriented from north or northwest China. The simulation of regional dust model also indicates the most possible source of the non-spherical particle is outflow of Asian dust.

In this paper, the optical properties such as backscatter ratio, depolarization ratio, lidar ratio and backscatter-related angstrom component α_{back} of dusts measured by lidar are reported. The lidar ratio of 355 nm S_{355} is about 32-72 sr. Most of the correlations between particle depolarization and α_{back} were found negatively correlated implying that the aerosol non-sphericity increased with increase in the aerosol size. If dust located in moist air, α_{back} is found may not change while particle depolarization decreases if relative humidity RH>60%.

2. METHODS

2.1 Lidar

The lidar site is installed at the weather observatory of the National Taiwan University (25°00'N, 121°32'E), which is located at the southwestern part of the Taipei Basin. During the Asian winter monsoon, the average prevailing wind direction in the Taipei Basin swings between the northeast and the east.

RCEC/ASNTU Lidar is a dual-wavelength Raman and Depolarization Lidar system (manufactured by Zenon SA, Greece). The lidar system employs the second and third harmonics of Nd-YAG laser at 532 nm and 355 nm. More details are provided in Table 1. This system is 24 hours operated to probe the atmosphere in the height range between 0.3 km and 8 km.

Table 1. Lidar Characteristics

Laser	Nd:YAG (Big-Sky CFR-400)
Wavelength	532/355 nm
Pulse energy	65/60 mJ
Repetition rate	20 Hz
Transient Record	12 bits A/D converter at 20 MHz and 250 MHz photon counting (Licel TR20-40)
Height Resolution	7.5 m
Telescope	diameter 40 cm, focal length 160 cm
Channels	532 (*S* and *P*), 355 nm, and 387 nm (nighttime only)

Aerosol backscattering ratio R_λ is define as:

$$R_\lambda(z) = 1 + \frac{\beta_a(\lambda, z)}{\beta_m(\lambda, z)} \quad (1)$$

For nighttime measurement, the calculation of R_{355} and lidar ratio S_{355} are basing on Raman inversion algorithm by Ansmann *et al*. [1]. For daytime measurement, the calculation of aerosol backscatter is using the Klett's method [2] with range-depended lidar ratio obtained from nighttime Raman measurements. In this study, the lidar ratio for wavelength 532 nm is set to S_{532}=S_{355}. For the cases that Raman signal is not available, a fix lidar ratio S_{355}=45 [3-5] was applied. The depolarization ratio is define as the ratio of the return light of perpendicular to parallel polarizations, as given by the following equation:

$$DP = P_\perp / P_\parallel \quad (2)$$

where $P_\perp$ and $P_\parallel$ are the integrated return power for parallel and perpendicular directions relative to the outgoing laser beam. The particle depolarization δ_p is expressed by the following equation:

$$\delta_p = (R \times DP - \delta_m)/(R+1) \quad (3)$$

The molecular depolarization ratio δ_m is given as 1.4% [6]. The backscatter-related Angstrom coefficient as α_{back} define in Eq.3 is the negative of the slope of β_a with wavelength in logarithmic scale.

$$\alpha_{back} = -\frac{d \ln \beta_a(\lambda)}{d \ln(\lambda)} \quad (4)$$

2.2 HYSPLIT Back-trajectory and Dust Model

HYSPLIT back-trajectory and an Asian dust model were applied to investigate the sources of those non-spherical layers.
(http://www.arl.noaa.gov/ready/hysplit4.html)
The regional dust model was developed based on the Taiwan Air Quality Model (TAQM), a regional chemistry and aerosol model, in which a dust module was incorporated in this study. TAQM was ported and modified from the San Joaquin Valley Air Quality Model (SAQM) developed for the California Air Resources Board. The updated TAQM uses non-hydrostatic meteorological data, and can be applied to simulate the time-varying three-dimensional distributions of trace gases and particles over the Asia. For more details please refer to Tsai et al. [7].

3. RESULTS AND DISCUSSIONS

During the sampling period (spring of 2004 and 2005), there are 124 lidar operation days available for depolarization calculation. Owing to weather condition, only 108 days are not full cloudy. Aerosols located above boundary layer are found to frequently exhibit larger depolarization properties than aerosols near surface ground. The occurrence frequency of daily maximum (hourly averaged) of total depolarization ratio below and above boundary layer is shown in Fig. 1. As shown in Fig. 1, for aerosol above boundary layer (dashed line), the depolarization ratio varies from 1% to 25% with mean value of DP=5.89±4.47%. More than 70% of the daily maximum total depolarization ratios for aerosol above boundary layer (dash line) are distributed between 3.5% and 7.5%, which is much larger than the depolarization for aerosol below boundary layer (solid line) implying intrinsic difference between aerosols below and above boundary. The observed dust depolarization ratio is similar to depolarization ratio of dust measured in Mainland China and Japan.

Fig. 2 shows the depolarization layers mainly distributed at heights between 1 km and 4 km. And, occasionally, we could found non-spherical particles descend from height more then 6 km to 3 km. The result of our dust model shows most of dust layer located between 1 km and 5 km over Taipei. Fig. 3a shows a lidar observed depolarization layer located at height between about 1 km and 4 km on 2005/4/3, whereas, dust model also shows a dust layer appears at similar height and time.

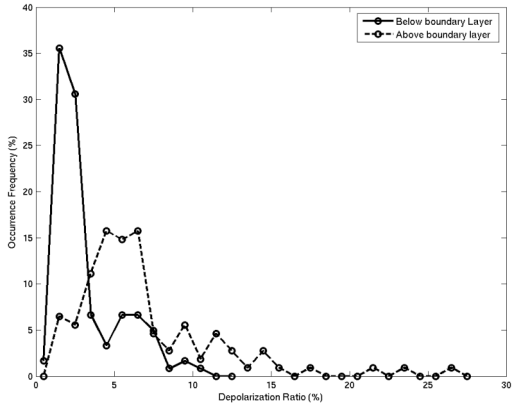

Fig. 1. Occurrence frequencies of depolarization ratio DP observed at height below boundary layer (solid line) or above boundary layer (dashed line).

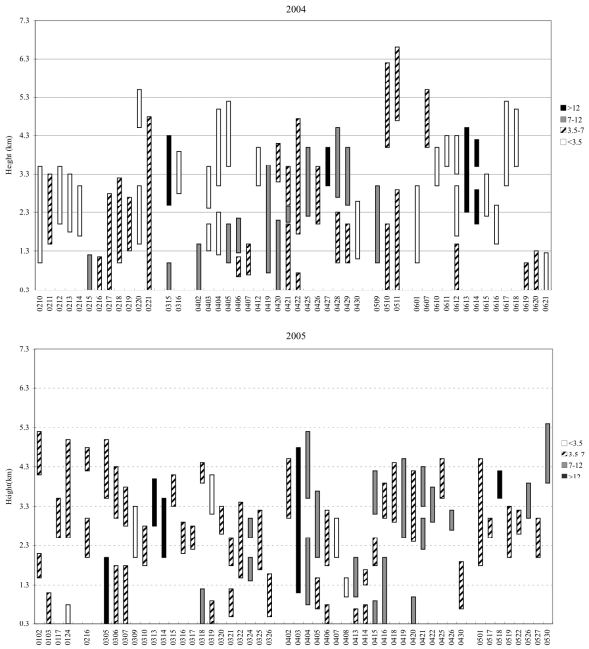

Fig. 2. Height distributions for aerosol with higher depolarization ratio (DP>3.5%) in the spring of 2004 and 2005.

Asian dust model and HYSPLIT back-trajectory analysis are applied to investigate the source of lidar observed depolarization layers. As shown in Fig. 4,

most of the air parcel could be tracked back to Northwest China. The closest FGGE dust reports along the trajectories are marked as (Δ). Very few HYSPLIT trajectories do not consist with dust Model simulation (not shown in Fig. 4) but seem to be oriented from South China or Southeast Asian implies Asian dust may not exactly transport along the trajectory of air parcel.

The lidar ratio for 355 nm S_{355} varies from 32~72 sr, which is close to that of Asian dust as reported in literatures. The relationship between the aerosol non-sphericity and the aerosol size was investigated by seeking the correlation between aerosol particle depolarization δ_p and backscatter-related angstrom component α_{back}. We found most of δ_p and α_{back} exhibit similar negative correlation. Fig. 5 shows the scatter plots of particle depolarization δ_p as a function of α_{back} at the edge (δ_p increase or decrease as variation of height) of depolarization layer for selected episodes. The particle depolarization δ_p, temperature and relative humidity for the dust layers shown in Fig. 5 are summarized in Table 2, where temperature and relative humidity are retrieved from radiosonde measurements. Fig. 5a shows the values of δ_p approximately linearly decreased from 25% to 2% with increasing of α_{back} from -0.7 to 1.5, which implying that the aerosol non-sphericity increased with increase in the aerosol size in that region.

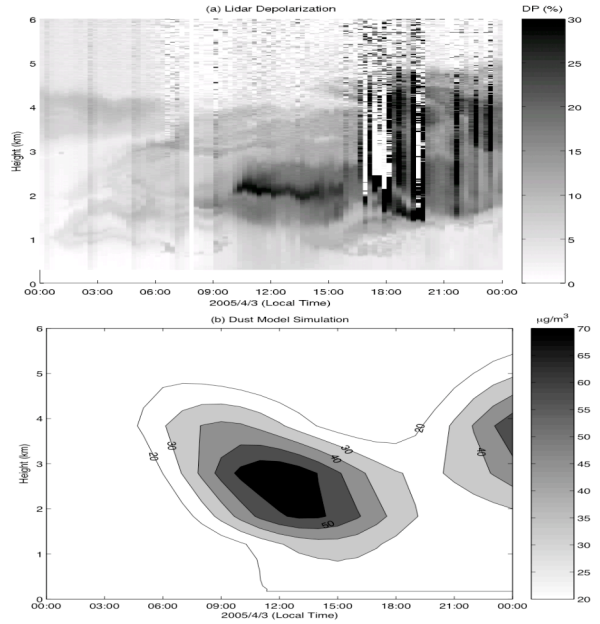

Fig. 3. A depolarization layer observed by lidar on 3rd April 2005 and the result of dust model simulation for the same day.

We also found δ_p may exhibit much different dependence with α_{back} if the maximum RH value exceeds about 60% (refer to Table 2). Which may imply the nonspherical particles changed their shape to spherical-like by uptaking water vapor at the higher RH or the proportion of nonspherical particles to the other low-depolarizing particles decreased within moist air [3, 8].

Ice crystal such as cirrus may exhibit different depolarization properties than dust. The correlation between δ_p and α_{back} for a cirrus measured on April 5, 2004 is also shown in Fig. 5a for comparison.

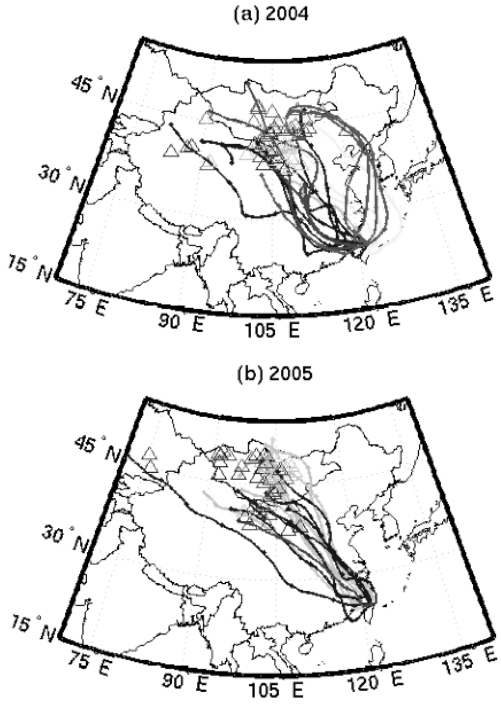

Fig. 4. Back-trajectories (HYSPLIT) for depolarization episodes shown in Fig. 2.

ACKNOWLEDGEMENTS

This work is supported by Research Center for Environmental Changes, Academia Sinica.

REFERENCES

1. Ansmann, A., U., *et al.*, Independent measurement of extinction and backscatter profile in cirrus clouds by using a combined Raman elastic-backscatter lidar, *Appl. Opt.*, Vol. 31, 7113-7131, 1992.

2. Klett, J.D., Stable analytic inversion solution for processing lidar returns, *Appl. Opt.*, Vol. 20, 211-220, 1981.

3. Sakai, T., et al., Case study of Raman lidar measurements of Asian dust events in 2000 and 2001 at Nagoya and Tsukuba, Japan, *Atmospheric Environment,*

Vol. 36, 5479–5489, 2002.

4. Liu *et al.*, Extinction-to-backscatter ratio of Asian dust observed with high-spectral-resolution lidar and Raman lidar, *Appl. Optics*, Vol. 41, 2760-2767, 2002.

5. Murayama, T., et al., Characterization of Asian dust and Siberian smoke with multi-wavelength Raman lidar over Tokyo, Japan in spring 2003, *Geophys. Res. Lett.*, Vol. 31 , L23103, 2004.

6. Young, A. T., Revised depolarization corrections for atmospheric extinction, *Appl. Opt.*, Vol. 19, 3427–3428, 1980.

7. Tsai, F., T.-H. Liu, S. C. Liu, T.-Y. Chen, T. L. Anderson, and S. J. Masonis, Model Simulation and Analysis of Coarse and Fine Particle Distributions During ACE-Asia, *J. Geophys. Res.*, 109, D19S20, doi: 10.1029/2003JD003665, 2004.

8. Krueger, B. J., V. H. Grassian, A. Laskin, and J. P. Cowin, The transformation of solid atmospheric particles into liquid droplets through heterogeneous chemistry: Laboratory insights into the processing of calcium containing mineral dust aerosol in the troposphere, *Geophys. Res. Lett.*, Vol. 30, 1148, doi: 10.1029/2002GL016563, 2003.

Table 2. The depolarization ratio of aerosol observed at height above boundary layer. The uncertainty of S_{355} is about 5 ~ 10 sr.

Date/Time	Height (km)	T (°C)	RH_{min} - RH_{max} (%)	Mean R_{532}	Maximum δ_p (%)	Mean α_{back}	Mean S_{355}	
2004/03/15 07:30	2.54 ~ 2.99	9.1 ~ 2.4	42.4 ~ 73.5	3.04	7	1.37	41	Fig. 5b
	2.99 ~ 3.75	6.2 ~ 2.7	41.5 ~ 42.4	2.28	12	1.37	46	Fig. 5a
2004/04/06 08:00	1.26 ~ 2.48	6.9 ~ 14.3	62.3 ~ 71.8	2.53	19	0.86	35	Fig. 5a
2004/04/19 20:00	1.91 ~ 2.44	13.2 ~ 8.2	34.1 ~ 68.4	2.08	10	1.46	39	Fig. 5b
2004/04/25 20:00	0.75 ~ 2.05	19.2 ~ 14.0	91.8 ~ 93.2	3.13	8	0.71	48	Fig. 5b
	2.05 ~ 3.38	14.0 ~ 7.5	64.0 ~ 72.2	2.45	12	1.05	43	Fig. 5a
2004/06/13 20:00	3.94 ~ 4.77	7.5 ~ 4.2	21.8 ~ 22.7	1.32	20	0.89	45	Fig. 5a
2004/05/09 20:00	1.16 ~ 1.90	19.6 ~ 18.7	6.14 ~ 89.2	2.70	11	0.39	39	Fig. 5b
	1.90 ~ 2.25	18.7 ~ 15.9	6.14 ~ 6.14	1.93	12	0.97	44	Fig. 5a
2005/04/03 08:00	0.75 ~ 1.21	13.1 -11.7	44.4 ~ 73.2	10.82	6	1.03	57	Fig. 5b
	1.21 ~ 2.48	11.7 ~ 5.2	22.6 ~ 44.4	4.94	21	0.96	46	Fig. 5a
2005/04/15 20:00	1.57 ~ 2.59	13.1 ~ 7.5	57.9 ~ 59.8	3.84	9	1.28	72	Fig. 5a
	2.59 ~ 3.00	7.5 ~ 5.61	56.7 ~ 86.8	3.02	7	1.19	65	Fig. 5b
2005/04/18 19:00	2.47 ~ 4.23	10.8 ~ 1.9	39.1 ~ 61.9	2.75	11	1.12	52	Fig. 5a
2005/04/21 20:00	1.06 ~ 1.74	20.6 ~ 16.4	51.1 ~ 61.1	5.50	10	1.33	45	Fig. 5a
	1.74 ~ 2.42	16.4 ~ 11.7	61.1 ~ 64.6	2.25	9	1.62	51	Fig. 5b
2005/04/26 20:00	3.00 ~ 3.48	7.49 ~ 4.68	64.2 ~ 69.8	1.51	25	0.71	62	Fig. 5a
2005/05/18 08:00	3.41 ~ 4.16	5.92 ~ 4.12	51.1 ~ 54.5	1.80	18	0.66	48	Fig. 5a
2004/04/05 05:00	7.42 ~ 8.43	-20 ~ -30	91.2 ~ 100.0	15.96	34	0.71	25	Cirrus

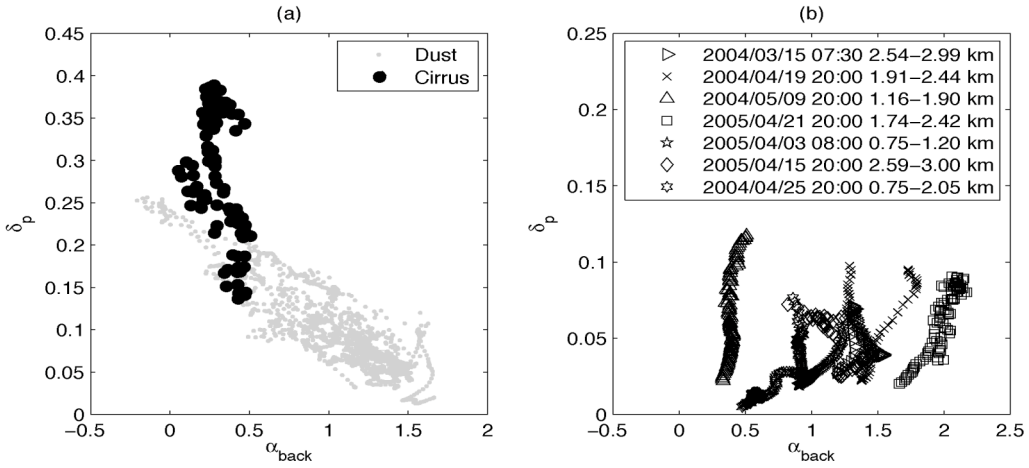

Fig. 5. Scatter diagram of aerosol particle depolarization ratio as a function of backscatter related angstrom exponent. A cirrus observed on April 5, 2004 is shown in Fig. 5a as solid circle.